CHIN. PHYS. LETT. Vol. 34, No. 4 (2017) 044204

Spatial-Variant Geometric Phase of Hybrid-Polarized Vector Optical Fields *

Yu Si(司宇)[1], Ling-Jun Kong(孔令军)[1], Yu Zhang(张瑜)[1], Zhi-Cheng Ren(任志成)[1], Yue Pan(潘岳)[1], Chenghou Tu(涂成厚)[1], Yongnan Li(李勇男)[1**], Hui-Tian Wang(王慧田)[1,2,3**]

[1]*School of Physics and Key Laboratory of Weak-Light Nonlinear Photonics, Nankai University, Tianjin 300071*
[2]*National Laboratory of Solid State Microstructures and School of Physics, Nanjing University, Nanjing 210093*
[3]*Collaborative Innovation Center of Advanced Microstructures, Nanjing 210093*

(Received 7 March 2017)

We investigate a novel spatial geometric phase of hybrid-polarized vector fields consisting of linear, elliptical and circular polarizations by Young's two-slit interferometer instead of the widely used Mach–Zehnder interferometer. This spatial geometric phase can be manipulated by engineering the spatial configuration of hybrid polarizations, and is directly related to the topological charge, the local states of polarization and the rotational symmetry of hybrid-polarized vector optical fields. The unique feature of geometric phase has implications in quantum information science as well as other physical systems such as electron vortex beams.

PACS: 42.25.Hz, 03.65.Vf, 42.25.Ja DOI: 10.1088/0256-307X/34/4/044204

Geometric phase, which was first pioneered in 1956[1] and rediscovered in 1984,[2] is a phase acquired when a system undergoes a cyclic adiabatic process. Such a phase difference is called geometric phase (Berry phase) because of dependence on the geometry of its parameter space. In a quantum system, the geometric phase results from the geometric properties of the parameter space of its Hamiltonian. Besides the quantum systems, the geometric phase also occurs in classical systems. The geometric phase, as a universal phenomenon, also occurs in nonadiabatic state changes[2,3] and even in noncyclic evolutions.[4,5] The geometric phase has many important applications such as quantum information[6,7] and quantum computation,[8−10] due to its robust feature.

The electric vector of a classical optical field is analogous to the wavefunction in a quantum system. Pancharatnam's early study on the interference of polarized light[1] was seminal to generalize the geometric phase. When the state of polarization (SoP) of an optical field is made to trace out a closed circuit on the Poincaré sphere[11] a geometric phase will be acquired and is equal to half the solid angle subtended by the closed circuit to the origin of the Poincaré sphere. The geometric phase in classical optics is of great importance[12] and has interesting applications.[13−16]

Most previous researches dealt with the geometric phase arising from the manipulation of optical fields with the spatially homogeneous SoP. Recently, there is an increasing interest in spatially structured optical fields, e.g. vortex optical fields carrying orbital angular momentum (OAM)[17] and vector optical fields with inhomogeneous SoP distribution.[18] Mode transformation of higher-order Laguerre-Gaussian fields carrying the OAM leads to a new geometric phase.[19,20] Higher-order Pancharatnam–Berry phase originating from the vector optical field is proportional to the total angular momentum [sum of SAM (spin angular momentum) and OAM].[21] Zhan *et al.*[22] have measured the spiral geometric phase using a Mach–Zehnder interferometer.

In this Letter, we explore the spatial geometric phase of hybrid-polarized vector optical fields (HP-VOFs) using the two-slit interference. By erasing the path information and controlling the local SoP distribution, we can manipulate the magnitude and sign of the geometric phase, which is insensitive to the dynamical phase.

We now consider a kind of HP-VOFs expressed as

$$|\Phi_m(\phi)\rangle = \frac{1}{\sqrt{2}} e^{jm\phi}|L_1\rangle + \frac{1}{\sqrt{2}} e^{-jm\phi}|L_2\rangle, \quad (1)$$

with $|L_1\rangle = \cos\phi_0|H\rangle + \sin\phi_0|V\rangle$ and $|L_2\rangle = -\sin\phi_0|H\rangle + \cos\phi_0|V\rangle$. $(|L_1\rangle, |L_2\rangle)$ are a pair of orthogonal unit base vectors and $(|H\rangle, |V\rangle)$ are also a pair of orthogonal unit base vectors in the horizontal and vertical directions. The phase factors $\exp(\pm jm\phi)$ indicate the vortex phases (carrying OAMs of $\pm m\hbar$ per photon, where the integer m is the topological charge and ϕ is the azimuth angle in the section of the optical field, respectively). Here ϕ_0, an angle formed by the horizontal direction, determines which pair of orthogonal linear polarizations will be selected as the basis. The HP-VOF in Eq. (1) is in fact a combination of a pair of orthogonal linearly polarized basis $(|L_1\rangle, |L_2\rangle)$ carrying the opposite OAMs. Of course, the HP-VOF in Eq. (1) can also be represented by a

*Supported by the National Natural Science Foundation of China under Grant Nos 11534006, 11674184 and 11374166, the Natural Science Foundation of Tianjin under Grant No 16JC2DJC31300, and Collaborative Innovation Center of Extreme Optics.
**Corresponding author. Email: htwang@nju.edu.cn; liyongnan@nankai.edu.cn
© 2017 Chinese Physical Society and IOP Publishing Ltd

pair of bases $(|H\rangle, |V\rangle)$ in Jones vectors as

$$|\Phi_m(\phi)\rangle = \frac{1}{\sqrt{2}} \begin{bmatrix} \cos\phi_0 e^{jm\phi} - \sin\phi_0 e^{-jm\phi} \\ \sin\phi_0 e^{jm\phi} + \cos\phi_0 e^{-jm\phi} \end{bmatrix}. \quad (2)$$

Based on the geometric representation of Poincaré sphere,[11] we can write the orthogonal basis as $|L_1\rangle = [S_1, S_2, S_3] = [\cos 2\phi_0, \sin 2\phi_0, 0]$ and $|L_2\rangle = [S_1, S_2, S_3] = [-\cos 2\phi_0, -\sin 2\phi_0, 0]$ in normalized Stokes parameters, respectively. In fact, a pair of basis $(|L_1\rangle, |L_2\rangle)$ correspond to a pair of antipodal points on Poincaré sphere Σ. Thus the SoPs of the HP-VOF in Eq. (1) or (2) can be written by the Poincaré's representation, i.e.,

$$\begin{bmatrix} S_1 \\ S_2 \\ S_3 \end{bmatrix} = \begin{bmatrix} -\cos(2m\phi)\sin(2\phi_0) \\ \cos(2m\phi)\cos(2\phi_0) \\ -\sin(2m\phi) \end{bmatrix}. \quad (3)$$

It is clear that the SoPs of the HP-VOF in Eq. (1) or (2) correspond to points with the coordinates on Σ,

$$(2\chi, 2\psi) = (-2m\phi, 2\phi_0 + \pi/2), \quad (4a)$$
$$(2\chi, 2\psi) = (2m\phi + \pi, 2\phi_0 - \pi/2). \quad (4b)$$

In fact, the two longitude lines $2\psi = 2\phi_0 \pm \pi/2$ form a circle passing through the north and south poles on Σ and this longitude circle plane is perpendicular to the diameter linking the two points (corresponding to $|L_1\rangle$ and $|L_2\rangle$) in the equator. All the SoPs of the HP-VOF in Eq. (1) or (2) lie on this longitude circle. One should point out that a rotation of ϕ about the field axis is equivalent to a rotation of $2\,m\phi$ in the longitude circle on Σ.

Milione *et al.*[21] investigated the higher-order geometric phase of the vector field as a whole during a cyclic transformation on the higher-order Poincaré sphere,[23] like the well-known geometric phase during a cyclic transformation on the stand Poincaré sphere. Here we are interested in the *space-variant* geometric phase of the HP-VOFs, which is completely different from Ref. [21]. In fact, such a space-variant geometric phase should be the relative geometric phase difference between any location and a certain reference point across the section of the HP-VOF. To find this space-variant geometric phase, we should review the non-cyclic polarization changes along the non-closed path on the stand Poincaré sphere.

Let us consider two fields $|A\rangle$ and $|B\rangle$, which may have different SoPs as

$$|A\rangle = \begin{bmatrix} A_x \\ A_y \end{bmatrix}, \quad |B\rangle = \begin{bmatrix} B_x \\ B_y \end{bmatrix} \quad (5)$$

with $|A_x|^2 + |A_y|^2 = |B_x|^2 + |B_y|^2 = 1$.

One main contribution of Pancharatnam facilitated the creation of Pancharatnam's connection, which is a criterion for two fields $|A\rangle$ and $|B\rangle$ with different SoPs. Pancharatnam's connection[24] requires that if $|A\rangle$ and $|B\rangle$ are in phase, their coherent superposition must have a maximal intensity, i.e., when

$$\langle A+B|A+B\rangle = \langle A|A\rangle + \langle B|B\rangle + 2\Re\mathfrak{e}\langle B|A\rangle \quad (6)$$

reaches the greatest value, we will have

$$\{\Im\mathfrak{m}\langle B|A\rangle = 0\} \cap \{\Re\mathfrak{e}\langle B|A\rangle > 0\}. \quad (7)$$

However, $|A\rangle$ and $|B\rangle$ are not always in phase. To find out the phase difference between $|A\rangle$ and $|B\rangle$, one can introduce an additional phase γ_{AB} into $|B\rangle$ $[|B\rangle \to |B'\rangle = \exp(j\gamma_{AB})|B\rangle]$, which can ensure $|A\rangle$ and $|B'\rangle$ to be in phase, requiring that

$$\{\Im\mathfrak{m}\langle B'|A\rangle = 0\} \cap \{\Re\mathfrak{e}\langle B'|A\rangle > 0\}. \quad (8)$$

The conditions allow to uniquely determine the phase difference γ_{AB}, which is considered as the non-cyclic geometric phase between $|A\rangle$ and $|B\rangle$, except when $|A\rangle$ and $|B\rangle$ are orthogonal. Importantly, van Dijk *et al.*[25] presented a geometric interpretation of Pancharatnam's connection: γ_{AB} is equal to half the solid angle Ω_{XAB} subtended by the geodesic triangle composed of the two Stokes vectors describing $|A\rangle$ and $|B\rangle$ as well as the Stokes vector as a reference state $|X\rangle$ on Σ ($\gamma_{AB} = \Omega_{XAB}/2$). Therefore, the non-cyclic geometric phase between $|A\rangle$ and $|B\rangle$ is equivalent to the geometric phase of the cycle subtended by the reference state $|X\rangle$ [for example, the point marked by the star in Fig. 1(b)] and the two states $|A\rangle$ and $|B\rangle$. In particular, one should point out that $|A\rangle$ and $|X\rangle$ are in phase, i.e., $\gamma_{XA} = 0$.

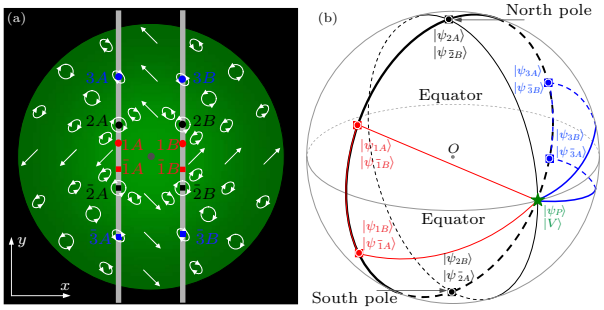

Fig. 1. (a) Configuration of the two-slit interference of the HP-VOF with $m = 1$ and $\phi_0 = 0$ as an example. (b) Geometric presentation of the spatial-variant geometric phase on Poincaré sphere.

For the HP-VOF in Eq. (1) or (2), its SoP distribution depends only on the azimuthal angle ϕ independent of the radial coordinate, so its geometric phase should also be a function of ϕ only. To find the space-variant geometric phase, without loss of generality, we choose the direction of $\phi = 0$ as a reference, there the local SoP is $|\Phi_m(0)\rangle = \cos(\phi_0 + \pi/4)|H\rangle + \sin(\phi_0 + \pi/4)|V\rangle$, with its Stokes parameters $[S_1, S_2, S_3] = [\cos(2\phi_0 + \pi/2), \sin(2\phi_0 + \pi/2), 0]$

and its spherical coordinates $(2\chi, 2\psi) = (0, 2\phi_0+\pi/2)$. Here ϕ_0 determines the SoP at the reference direction of $\phi = 0$.

As configuration of two-slit interference shown in Fig. 1(a), an HP-VOF in Eq. (1) or (2) falls on the two parallel slits A and B placed symmetrically about the origin. The fields transmitted through A and B, as two secondary *line* sources, interfere mutually in the far-field, and the interference pattern is recorded by a CCD camera. The separation b between A and B is much larger than their width a and is much smaller than the distance d of the observation plane from the xy (slits) plane. The SoPs inside A and B can be considered to be homogeneous in the x direction while are space-variant in the y direction. In Fig. 1(a), we mark six pairs of points inside A and B, where the paired points $[NA, NB]$ and $[\overline{N}A, \overline{N}B]$ (where $N = 1, 2, 3$) are the mirror symmetry with respect to the x axis, respectively.

The photon state through $A(B)$ can be described by its transverse component of wave vector $|k_A\rangle$ ($|k_B\rangle$) and its SoP $|\psi_A\rangle$ ($|\psi_B\rangle$). Thus the superposition state on the observation plane should be[26]

$$|\psi_0\rangle = |\psi_A\rangle|k_A\rangle + |\psi_B\rangle|k_B\rangle. \tag{9}$$

We introduce an operator $\hat{P}_x = \hat{I} \otimes |x\rangle\langle x|$, which projects the path state into the position state $|x\rangle$ on the observation plane. With the position representation of the wave-vector eigenfunction, $\langle x|k\rangle = e^{jkx}/\sqrt{2\pi}$, the probability distribution $P_0(x)$ on the observation is given by

$$P_0(x) = \langle\psi_0|\hat{P}_x|\psi_0\rangle \propto 1 + V_0\cos(kx - \delta_0), \tag{10}$$

where $k = k_B - k_A = 2\pi d/\lambda L$ (λ is the wavelength of light). The visibility V_0 and the phase shift δ_0 are given by $V_0 = |\langle\psi_B|\psi_A\rangle|$ and $\delta_0 = \arg\langle\psi_B|\psi_A\rangle$, respectively. Here δ_0 is in fact the Pancharatnam phase[24] from $|\psi_B\rangle$ to $|\psi_A\rangle$.

To erase the path information, a linear polarizer (with an orientation angle θ with respect to the x direction) is used to project the SoP into $|\psi_P\rangle = \cos\theta|H\rangle + \sin\theta|V\rangle$. The state behind the linear polarizer should be $|\psi_e\rangle = |\psi_P\rangle\langle\psi_P||\psi_0\rangle$. The probability distribution on the observation plane, $P_e(x)$, is given by

$$P_e(x) = \langle\psi_e|\hat{P}_x|\psi_e\rangle \propto 1 + V_e\cos(kx - \delta_0 - \delta_g), \tag{11}$$

where the visibility V_e and the phase shift δ_g are given by

$$V_e = \frac{2|\langle\psi_P|\psi_A\rangle||\langle\psi_P|\psi_B\rangle|}{|\langle\psi_P|\psi_A\rangle|^2 + |\langle\psi_P|\psi_B\rangle|^2}, \tag{12}$$

$$\delta_g = \arg[\langle\psi_B|\psi_P\rangle\langle\psi_P|\psi_A\rangle\langle\psi_A|\psi_B\rangle]. \tag{13}$$

Here δ_g is the geometric phase in the two-slit interference and can be interpreted by Poincaré sphere as shown in Fig. 1(b); δ_g is equal to half the solid angle surrounded by the three points on Σ, $|\psi_B\rangle$, $|\psi_P\rangle$ and $|\psi_A\rangle$,

$$\delta_g(\psi_B, \psi_P, \psi_A) = \frac{1}{2}\Omega(\psi_B, \psi_P, \psi_A). \tag{14}$$

The sign of δ_g depends on the order of the three SoPs. Based on the definition of Poincaré sphere,[11] we obtain the ratio of the Stokes parameters (S_1 and S_2) of the HP-VOF in Eq. (1) or (2) to be $S_2/S_1 = \tan(2\phi_0 \pm \pi/2)$, which is a constant independent of the spatial coordinate. Therefore, the SoPs at all the positions cross the section of the HP-VOF are located at a longitude circle (composed of a longitude line with $2\phi_0 + \pi/2$ and its anti-longitude line with $2\phi_0 - \pi/2$) on Σ.

For the HP-VOF with $\phi_0 = 0$, as an example shown in Fig. 1, all the SoPs are located at a longitude circle composed of the longitude line with $\pi/2$ (shown by the black thick-solid semicircle) and its anti-longitude line with $-\pi/2$ (shown by the black thick-dashed semicircle) on Σ in Fig. 1(b). The SoPs at $1A$ and $1B$ points in Fig. 1(a), $|\psi_{1A}\rangle$ and $|\psi_{1B}\rangle$, are the right-handed (RH) and left-handed (LH) elliptical polarizations with the same orientation and ellipticity, corresponding to a pair of points at the black thick-solid longitude line on Σ and exhibit the mirror symmetry with respect to the equator, as shown in Fig. 1(b). The SoPs at $2A$ and $2B$ points in Fig. 1(a), $|\psi_{2A}\rangle$ and $|\psi_{2B}\rangle$, are the RH and LH circular polarizations, corresponding to the north and south poles on Σ, as shown in Fig. 1(b). The SoPs at $3A$ and $3B$ points in Fig. 1(a), $|\psi_{3A}\rangle$ and $|\psi_{3B}\rangle$, are the RH and LH elliptical polarizations with the same orientation and ellipticity, corresponding to a pair of points at the black thick-dashed longitude line on Σ and exhibit the mirror symmetry with respect to the equator, as shown in Fig. 1(b). In particular, one should point out that the SoP at the NA (NB) point is the same as that at the $\overline{N}B$ ($\overline{N}A$) point ($N = 1, 2, 3$).

When the linear polarizer is chosen to be the vertical polarization $|\psi_P\rangle = |V\rangle$ (i.e. $\theta = \pi/2$), which corresponds to the point (shown by the star) on the equator of Σ [Fig. 1(b)], the geometric phase between $|\psi_{1A}\rangle$ and $|\psi_{1B}\rangle$ [or $|\psi_{\overline{1}A}\rangle$ and $|\psi_{\overline{1}B}\rangle$] is proportional to the solid angle $\Omega(\psi_{1B}, \psi_P, \psi_{1A})$ [or $\Omega(\psi_{\overline{1}B}, \psi_P, \psi_{\overline{1}A})$] of the geodesic triangle (surrounded by the thin red-solid lines) connecting the states $|\psi_{1B}\rangle$, $|\psi_P\rangle$ and $|\psi_{1A}\rangle$ [or $|\psi_{\overline{1}B}\rangle$, $|\psi_P\rangle$ and $|\psi_{\overline{1}A}\rangle$] on Σ [Fig. 1(b)].

Due to the vector character of the HP-VOF, the input SoPs continuously change with y along the slits. Correspondingly, the states $|\psi_A\rangle$ and $|\psi_B\rangle$ inside the two slits gradually move along the prime meridian on Σ. Therefore, the space-variant polarization states result in space-variant geometric phase, which is given

from Eq. (13) by

$$\tan\delta_g = \frac{\cos[2(\theta-\phi_0)]\sin[m(\varphi_A-\varphi_B)]}{\cos[m(\varphi_A-\varphi_B)]+\sin[2(\theta-\phi_0)]}, \quad (15)$$

where $\varphi_A = \arctan(-2y/b)$ and $\varphi_B = \arctan(2y/b)$ describe the position coordinates inside A and B in the y direction.

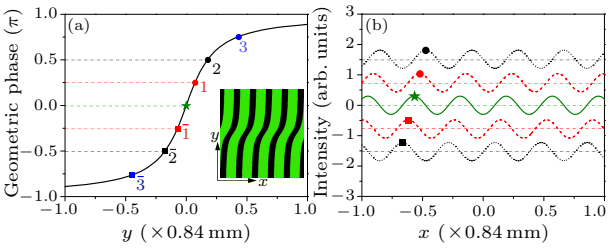

Fig. 2. (a) Dependence of the geometric phase on the y coordinate. Inset: an example of the interference pattern. (b) Intensity distributions along the x direction for five different y coordinates by setting $\theta = \pi/2$, $\phi_0 = 0$ and $m = 1$.

We can see from Eq. (15) that the geometric phase is determined by the five parameters of m, ϕ_0, y, b and θ. Here m and ϕ_0 determine what HP-VOF is; θ determines what linear polarizer is used to the projection of SoPs. To intuitively depict the space-variant geometric phase, we perform the simulations, as shown in Fig. 2. For the HP-VOF with $m = 1$ and $\phi_0 = 0$, when a vertical linear polarizer $|\psi_P\rangle = |V\rangle$ ($\theta = \pi/2$) is used to the projection of SoPs, the dependence of δ_g on y can be obtained for a given b, as shown in Fig. 2(a). The geometric phase δ_g is positive when $y > 0$, while the geometric phase δ_g is negative when $y < 0$.

Figure 2(b) illustrates the dependence of the intensity on the x coordinate for five fixed y coordinates, which shows clearly the interference fringe patterns. The periods and the visibility of the fringes are independent of the y coordinate, but the fringes are bent and not as straight as the traditional two-slit interference, due to the presence of the spatial-variant geometric phase instead of the dynamical phase. The fringes exhibit a shift, with the change of the y coordinate, in detail, the shift is toward the $+x$ direction in the region of $y > 0$ while the $-x$ direction in the region of $y < 0$. The fringe shift is proportional to the geometric phase δ_g. We can give the fringe shift from Eq. (11) as follows:

$$\Delta x = \Lambda(\delta_g/2\phi_0), \quad (16)$$

where Λ is the period of the fringes on the screen. The property of fringe patterns we just mentioned is in agreement with the expression in Eq. (16).

We now explore experimentally Young's two-slit interference of the HP-VOFs. A 532-nm laser as a light source is used to create the HP-VOFs in Eq. (1) or (2), using the method presented in Ref. [27]. The created HP-VOF is incident normally on the two slits with the same slit width ($a = 0.2$ mm) and the separation of the slits ($b = 0.8$ mm). A CCD camera placed in the observation plane, which has a distance $d = 500$ mm from the slits, is used to acquire the interference pattern. A polarizer, which is attached on a rotatable stage for adjusting θ, is inserted between the slits and the CCD.

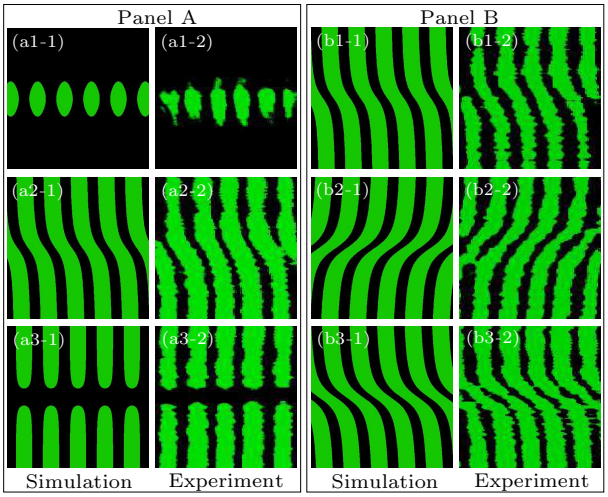

Fig. 3. Panel A: the interference patterns of the hybrid vector optical fields by setting $\theta = \pi/2$ and $m = 1$. The first and second rows give the theoretical and experimental results, (a1-1) and (a1-2) $\phi_0 = \pi/4$, (a2-1) and (a2-2) $\phi_0 = \pi/2$, and (a3-1) and (a3-2) $\phi_0 = 3\pi/4$. Panel B: the interference patterns of the hybrid vector optical fields by setting $\theta = \pi/2$ and $\theta = 0$. The first and second rows give the theoretical and experimental results, (b1-1) and (b1-2) $m = -1$, (b2-1) and (b2-2) $m = 2$, and (b3-1) and (b3-2) $m = -2$. All the pictures have the same dimensions of 1.68×1.68 mm^2. The x and y axes are along the horizontal and vertical directions, respectively.

Figure 3 shows the simulated and measured interference patterns of the HP-VOFs for different cases. In panel A, all the cases are set as $\theta = \pi/2$, implying that a vertical polarizer is used to project the SoPs, and the three HP-VOFs have the same topological charge of $m = 1$. Three different values of $\phi_0 = \pi/4$, $\pi/2$ and $3\pi/4$ correspond to three pairs of different base vectors to be chosen for generating three different HP-VOFs. Clearly, the fringes of two HP-VOFs with $\phi_0 = \pi/4$ [Figs. 3(a1-1) and 3(a1-2)] and $\phi_0 = 3\pi/4$ [Figs. 3(a3-1) and 3(a3-2)] are symmetrical about both x and y axes. For the HP-VOF with $\phi_0 = \pi/4$ (or $\phi_0 = 3\pi/4$), the states $|\psi_A\rangle$ and $|\psi_B\rangle$ move along the prime meridian circle (shown by thin-black solid and dashed semicircles) on Σ, which passes through the state $|V\rangle$ on Σ [Fig. 1(b)]. In this case, therefore, the geometric phase is zero and the interference patterns [Figs. 3(a1) and 3(a3)] are the same as the local linearly-polarized vector fields.[28] Panel B shows the interference patterns of the HP-VOFs with different topological charges. We can find

that the slope of fringes becomes larger, that is to say, the gradient of geometric phase enlarges, as the topological charge m increases. Hence the magnitude and sign of the geometric phase can be controlled by the topological charge of the HP-VOF.

The spatial geometric phase is the unique feature of the HP-VOF, which is quite different from the well-known geometric phase associated with homogeneously polarized light. Recently, the geometric phase for a non-cyclic polarization change, which means that the initial and final states are different (corresponding to a non-closed path on Σ), has been studied.[5] The spatial geometric phase should be a general feature of the vector optical fields.

In conclusion, we have theoretically and experimentally investigated the spatial geometric phase of HP-VOFs. The geometric phase has found novel applications in quantum information science due to its robustness and distinction from a dynamic phase. The vector fields correspond to the four-dimensional quantum states encoded in the polarization and OAM of a single photon.[29,30] The spatial geometric phase may lead to new applications, such as in photonic analog of a topological phase gate,[31] geometric quantum computation,[32,33] vector vortex beams,[21] and spin-orbit conversion of vortex electron beams.[34]

References

[1] Pancharatnam S 1956 *Proc. Indian. Acad. Sci.* A **44** 247
[2] Berry M V 1984 *Proc. R. Soc. London Ser.* A **392** 45
[3] Anandan J 1992 *Nature* **360** 307
[4] Wang X B and Matsumoto K 2001 *Phys. Rev. Lett.* **87** 097901
[5] Morinaga A, Monma A, Honda K and Kitano M 2007 *Phys. Rev.* A **76** 052109
[6] van Dijk T, Schouten H F, Ubachs W and Visser T D 2010 *Opt. Express* **18** 10796
[7] Leek P J, Fink J M, Blais A, Bianchetti R, Gö ppl M, Gambetta J M, Schuster D I, Frunzio L, Schoelkopf R J and Wallraff A 2007 *Science* **318** 1889
[8] Blais A, Gambetta J, Wallraff A, Schuster D I, Girvin S M, Devoret M H and Schoelkopf R J 2007 *Phys. Rev.* A **75** 032329
[9] Zhu S L and Wang Z D 2002 *Phys. Rev. Lett.* **89** 097902
[10] Jones J A, Vedral V, Ekert A and Castagnoli G 2000 *Nature* **403** 869
[11] Born M and Wolf E 1999 *Principles of Optics* 7th edn (Cambridge: Cambridge University Press)
[12] Kurzynowski P, Wozniak W A and Szarycz M 2011 *J. Opt. Soc. Am.* A **28** 475
[13] Wozniak W A and Kurzynowski P 2012 *J. Opt. Soc. Am.* A **29** 2226
[14] Watkins L R and Derbois M 2012 *Appl. Opt.* **51** 5060
[15] Naik D N, Ezawa T, Miyamoto Y and Takeda M 2009 *Opt. Express* **17** 10633
[16] Roy M, Schmit J and Hariharan P 2009 *Opt. Express* **17** 4495
[17] Yao A M andPadgett M J 2011 *Adv. Opt. Photon.* **3** 161
[18] Zhan Q 2009 *Adv. Opt. Photon.* **1** 1
[19] Galvez E J, Crawford P R, Sztul H I, Pysher M J, Haglin P J and Williams R E 2003 *Phys. Rev. Lett.* **90** 203901
[20] Habraken S J M and Nienhuis G 2010 *Opt. Lett.* **35** 3535
[21] Milione G, Evans S, Nolan D A and Alfano R R 2012 *Phys. Rev. Lett.* **108** 190401
[22] Zhan Q and Leger J R 2002 *Opt. Commun.* **213** 241
[23] Milione G, Sztul H I, Nolan D A and Alfano R R 2011 *Phys. Rev. Lett.* **107** 053601
[24] Berry M V 1987 *J. Mod. Opt.* **34** 1401
[25] van Dijk T, Schouten H F and Visser T D 2010 *J. Opt. Soc. Am.* A **27** 1972
[26] Kobayashi H, Tamate S, Nakanishi T, Sugiyama K and Kitano M 2011 *J. Phys. Soc. Jpn.* **80** 034401
[27] Wang X L, Li Y N, Chen J, Guo C S, Ding J P and Wang H T 2010 *Opt. Express* **18** 10786
[28] Li Y N, Wang X L, Zhao H, Kong L J, Lou K, Gu B, Tu C H and Wang H T 2012 *Opt. Lett.* **37** 1790
[29] Barreiro J T, Wei T C and Kwiat P G 2008 *Nat. Phys.* **4** 282
[30] Nagali E, Sansoni L, Marrucci L, Santamato E and Sciarrino F 2010 *Phys. Rev.* A **81** 052317
[31] Leibfried D, DeMarco B, Meyer V, Lucas D, Barrett M, Britton J, Itano W M, Jelenkovic B, Langer C, Rosenband T and Wineland D J 2003 *Nature* **422** 412
[32] Wang Z S, Liu G Q and Ji Y H 2009 *Phys. Rev.* A **79** 054301
[33] Oxman L E and Khoury A Z 2011 *Phys. Rev. Lett.* **106** 240503
[34] Karimi E, Marrucci L, Grillo V and Santamato E 2012 *Phys. Rev. Lett.* **108** 044801